

INTEGRAL TRANSFORM ANALYSIS OF CONDUCTION HEAT TRANSFER IN SPHEROIDAL SOLIDS

Simone de Aviz Cardoso

Chemical and Food Engineering Department, CT, Universidade Federal do Pará, Campus Universitário do Guamá, Rua Augusto Corrêa, 01, 66075-110, Belém, PA

Emanuel Negrão Macêdo

Chemical and Food Engineering Department, CT, Universidade Federal do Pará, Campus Universitário do Guamá, Rua Augusto Corrêa, 01, 66075-110, Belém, PA

João Nazareno Nonato Quaresma

Chemical and Food Engineering Department, CT, Universidade Federal do Pará, Campus Universitário do Guamá, Rua Augusto Corrêa, 01, 66075-110, Belém, PA
quaresma@ufpa.br

Abstract. *The temperature field in conduction heat transfer within an spheroidal solid is analytically analyzed by using the Generalized Integral Transform Technique (GITT) methodology. The mathematical modeling of the problem is done by assuming that the solid surface can be described by a general function, in such way the cylindrical coordinates system is employed to avoid those ones that lead to models of difficulty solutions. A computational code was developed to compute the temperature field within the solid of different geometric configurations, and the results were then compared with those previously reported in the literature for typical situations.*

Keywords. *Conduction heat transfer, Spheroidal solids, Integral transform.*

1. Introduction

Conduction heat transfer in spheroidal solids is frequently found in applications involving the processing of foods and grains such as in the drying of fruits and seeds, to name a few. The mathematical modeling of this problem is done by writing the heat conduction equation in coordinates systems that lead to more involved solutions. The classical paper of Haji-Sheikh and Sparrow (1966) shows the analysis of heat conduction in a prolate spheroidal solid, in which the solution is expressed in terms of coupled spherical Bessel and Legendre functions. Along the years many works have treated this problem using analytical or numerical schemes to solve the heat diffusion equation (Haji-Sheikh, 1986; Lima and Nebra, 1999).

The present work in order to avoid the analysis pointed out in the papers cited above and to handle more complex geometric configurations, assumes that the solid surface can be described by a general function, in such way the cylindrical coordinates system is employed to modeling the problem, and consequently the ideas of the well-established Generalized Integral Transform Technique (GITT) for problems in irregular domains (Aparecido et al, 1989; Aparecido and Cotta, 1990; Cotta, 1993 and 1994; Pérez Guerrero et al, 2000 and Chaves et al, 2001) are then used to obtain the solution of this more general formulation. This spectral-type approach is based on eigenfunction expansions yielding to solutions where the most features are the automatic and straightforward global error control and, an only mild cost increase in overall computational effort for multidimensional situations. Due to its analytical and hybrid natures, this scheme has been well indicated for benchmarking purposes and for the validation of different numerical methods in many classes of heat, mass and fluid flow problems.

Numerical results for the temperature field are obtained, considering different geometric configurations subjected to a first kind boundary condition at the surface, which are compared with those previously reported in the literature for typical situations.

2. Analysis

We consider transient heat conduction in spheroidal solids in which their surfaces are described for a general function and are subjected to a first kind boundary condition as shown in Fig. (1). Assuming constant thermophysical properties and no internal heat generation, the heat diffusion equation in cylindrical coordinates system in dimensionless form is written as follows:

$$\frac{\partial \theta(R, Z, \tau)}{\partial \tau} = \frac{1}{R} \frac{\partial}{\partial R} \left[R \frac{\partial \theta(R, Z, \tau)}{\partial R} \right] + \frac{\partial^2 \theta(R, Z, \tau)}{\partial Z^2}, \quad \text{in } 0 < Z < 1, \quad 0 < R < R_w(Z), \quad \tau > 0 \quad (1a)$$

subjected to the initial and boundary conditions:

$$\theta(R, Z, 0) = 1 \quad (1b)$$

$$\frac{\partial \theta(0, Z, \tau)}{\partial R} = 0, \quad \theta(R_w(Z), Z, \tau) = 0, \quad 0 < Z < 1, \quad \tau > 0 \quad (1c,d)$$

$$\frac{\partial \theta(R, 0, \tau)}{\partial Z} = 0, \quad \theta(R, 1, \tau) = 0, \quad 0 < R < R_w(Z), \quad \tau > 0 \quad (1e,f)$$

where the following dimensionless variables are defined:

$$R = r/L_2, \quad Z = z/L_2, \quad \tau = \alpha t/L_2^2, \quad \theta(R, Z, \tau) = \frac{T(r, z, t) - T_s}{T_0 - T_s}, \quad \gamma = L_1/L_2, \quad R_w(Z) = r_w(z)/L_2 = \gamma \sqrt{1 - Z^2} \quad (2a-f)$$

The dimensionless variable $R_w(Z)$ describes a general function to represent the solid surface, and for typical situations values for the aspect ratio γ are taken as:

$$\begin{cases} \gamma = 1, & \text{for spherical solid} \\ 0 < \gamma < 1, & \text{for prolate solid} \\ \gamma > 1, & \text{for oblate solid} \end{cases} \quad (3a-c)$$

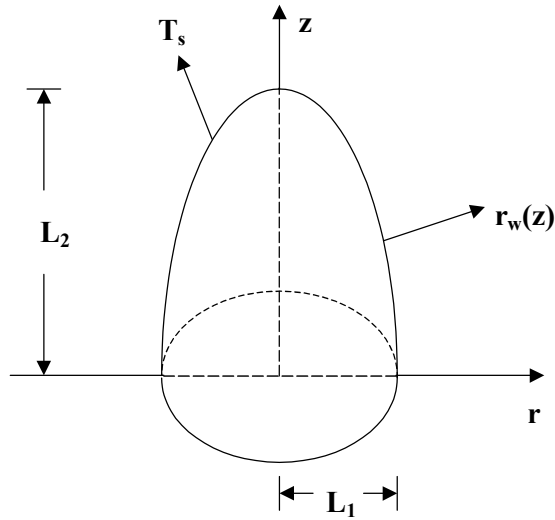


Figure 1. Geometry and coordinate system for heat conduction in spheroidal solids.

2.1. Solution methodology

Following the formalism in the GITT approach to handle problems in irregular domains (Cotta, 1993 and 1994), to construct the eigenfunctions expansion, the auxiliary eigenvalue problems are selected as:

- radial direction:

$$\frac{d}{dR} \left[R \frac{d\psi_i(R; Z)}{dR} \right] + \mu_i^2(Z) R \psi_i(R; Z) = 0, \quad \text{in } 0 < R < R_w(Z) \quad (4a)$$

$$\frac{d\psi_i(0; Z)}{dR} = 0, \quad \psi_i(R_w(Z); Z) = 0 \quad (4b,c)$$

where Z is just a parameter in the problem (4) above.

The eigenfunctions and the transcendental expression to calculate the eigenvalues are given, respectively, by:

$$\psi_i(R; Z) = J_0(\mu_i(Z)R), \quad J_0(\mu_i(Z)R_w(Z)) = 0 \quad \text{or} \quad J_0(\beta_i) = 0, \quad \mu_i(Z) = \beta_i / R_w(Z), \quad i = 1, 2, 3, \dots \quad (4d-g)$$

The eigenfunctions of this eigenvalue problem enjoy the following orthogonality property:

$$\int_0^{R_w(Z)} R \psi_i(R; Z) \psi_j(R; Z) dR = \begin{cases} 0, & i \neq j \\ N_i(Z), & i = j \end{cases} \quad (4h)$$

and the normalization integral is defined as:

$$N_i(Z) = \int_0^{R_w(Z)} R \psi_i^2(R; Z) dR = \frac{R_w^2(Z)}{2} J_1^2(\beta_i) \quad (4i)$$

- axial direction:

$$\frac{d^2 \phi_m(Z)}{dZ^2} + \lambda_m^2 \phi_m(Z) = 0, \quad \text{in } 0 < Z < 1 \quad (5a)$$

$$\frac{d\phi_m(0)}{dZ} = 0, \quad \phi_m(1) = 0 \quad (5b,c)$$

Problem (5) above is analytically solved to give the eigenfunctions and the eigenvalues, respectively, by:

$$\phi_m(Z) = \cos(\lambda_m Z), \quad \lambda_m = (2m - 1)\pi / 2, \quad m = 1, 2, 3, \dots \quad (5d,e)$$

The orthogonality property for this eigenvalue problem is given as:

$$\int_0^1 \phi_m(Z) \phi_n(Z) dZ = \begin{cases} 0, & m \neq n \\ M_m, & m = n \end{cases} \quad (5f)$$

and the normalization integral is calculated from:

$$M_m = \int_0^1 \phi_m^2(Z) dZ = \frac{1}{2} \quad (5g)$$

The problems given by Eqs. (4) and (5) allow the definition of the following integral-transform pair:

$$\tilde{\theta}_{im}(\tau) = \int_0^1 \int_0^{R_w(Z)} \frac{R \psi_i(R; Z) \phi_m(Z) \theta(R, Z, \tau)}{N_i(Z) M_m} dR dZ, \quad \text{transform} \quad (6)$$

$$\theta(R, Z, \tau) = \sum_{i=1}^{\infty} \sum_{m=1}^{\infty} \psi_i(R; Z) \phi_m(Z) \tilde{\theta}_{im}(\tau), \quad \text{inversion} \quad (7)$$

Equation (1a) is now integral transformed through the operator $\int_0^1 \int_0^{R_w(Z)} \{R \psi_i(R; Z) \phi_m(Z) / [N_i(Z) M_m]\} dR dZ$, to yield the following coupled system of transformed ordinary differential equations:

$$\frac{d\tilde{\theta}_{im}(\tau)}{d\tau} + \sum_{j=1}^{\infty} \sum_{n=1}^{\infty} A_{ijmn} \tilde{\theta}_{jn}(\tau) = 0 \quad (8)$$

The initial condition, Eq. (1b), is similarly integral transformed to provide:

$$\tilde{\theta}_{im}(0) = \tilde{f}_{im} = \int_0^1 \int_0^{R_w(Z)} \frac{R \psi_i(R; Z) \phi_m(Z)}{N_i(Z) M_m} dR dZ \quad (9)$$

where the coefficient in Eq. (8) is given by:

$$A_{ijmn} = \frac{\delta_{ij}\beta_i^2}{M_m} \int_0^1 \frac{\varphi_m(Z)\varphi_n(Z)}{R_w^2(Z)} dZ + \delta_{ij}\delta_{mn}\lambda_m^2 - \int_0^1 \int_0^{R_w(Z)} \frac{R\psi_i(R;Z) \frac{\partial^2 \psi_j(R;Z)}{\partial Z^2} \varphi_m(Z)\varphi_n(Z)}{N_i(Z)M_m} dRdZ$$

$$- 2 \int_0^1 \int_0^{R_w(Z)} \frac{R\psi_i(R;Z) \frac{\partial \psi_j(R;Z)}{\partial Z} \varphi_m(Z) \frac{d\varphi_n(Z)}{dZ}}{N_i(Z)M_m} dRdZ$$
(10a)

and,

$$\delta_{ij} = \begin{cases} 0, & i \neq j \\ 1, & i = j \end{cases}, \quad \delta_{mn} = \begin{cases} 0, & m \neq n \\ 1, & m = n \end{cases}$$
(10b)

In Eq. (8) each summation is associated with the eigenfunction expansion in a corresponding spatial coordinate, for computational purposes, the series solution given by Eq. (8) is, in general, truncated to a finite number of terms in order to compute the potential $\theta(R,Z,\tau)$. The solution convergence is verified by comparing the values for the potential obtained with the truncated series for different numbers of retained terms. Such number of terms is commonly user-supplied and even taken as the same for each summation.

Then, the indices i and m related to the temperature field are reorganized into the single index p , while the indices j and n are collapsed into the new index q . The associated double sums are then rewritten as:

$$\sum_{i=1}^N \sum_{m=1}^{N^*} \rightarrow \sum_{p=1}^{NT} \quad ; \quad \sum_{j=1}^N \sum_{n=1}^{N^*} \rightarrow \sum_{q=1}^{NT}$$
(11a,b)

where

$$i = \text{int}[(p-1)/N] + 1, j = \text{int}[(q-1)/N^*] + 1, m = p - (i-1)N \text{ and } n = q - (j-1)N^*$$
(11c-f)

The truncated version of system (8) is now rewritten in terms of these new indices as:

$$\frac{d\tilde{\theta}_p(\tau)}{d\tau} + \sum_{p=1}^{NT} A_{pq} \tilde{\theta}_q(\tau) = 0, \quad p = 1, 2, \dots, N \times N^*; q = 1, 2, \dots, N \times N^*$$
(12a)

$$\tilde{\theta}_p(0) = \tilde{f}_p$$
(12b)

The coupled system of ordinary differential equations (12) is solved by efficient numerical algorithms for initial value problems, such as in subroutine IVPAG from the IMSL package (1991), with high accuracy. Then, after the transformed potentials are obtained, quantities of practical interest are determined from the analytic inversion formula (7), such as the dimensionless average temperature

$$\theta_{av}(\tau) = \frac{1}{A_c} \int_{A_c} \theta(R, Z, \tau) dA = \frac{3}{\gamma^2} \int_0^1 \int_0^{R_w(Z)} R\theta(R, Z, \tau) dRdZ$$
(13a)

or

$$\theta_{av}(\tau) = \frac{3}{\gamma^2} \sum_{i=1}^N \sum_{m=1}^{N^*} \tilde{g}_{im} \tilde{\theta}_{im}(\tau), \quad \tilde{g}_{im} = \int_0^1 \int_0^{R_w(Z)} R\psi_i(R;Z)\varphi_m(Z) dRdZ$$
(13b,c)

Equation (13b) is then rewritten in terms of the new indices according to Eqs. (1), to yield

$$\theta_{av}(\tau) = \frac{3}{\gamma^2} \sum_{p=1}^{NT} \tilde{g}_p \tilde{\theta}_p(\tau)$$
(14)

3. Results and discussion

Numerical results for the temperature field and average temperature were produced for different values of aspect ratio, namely $\gamma^{-1} = 0.5; 1.0; 2.0$ and 5.0 , within the spheroidal solid. The computational code was developed in FORTRAN 90/95 programming language and implemented on a PENTIUM-IV 1.3 GHz computer. The routine DIVPAG from IMSL Library (1991) was used to numerically handled the truncated version of the system of ordinary differential equations (12), with a relative error target of 10^{-7} prescribed by the user, for the transformed potentials.

First, Tables (1) to (3) show the convergence behavior of the temperature field at the center ($R = 0, Z = 0$) and at the focal point ($R = L, Z = 0$ for $\gamma^{-1} = 0.5$ and $R = 0, Z = L$ for $\gamma^{-1} = 2.0$) of the spheroidal solid and the convergence behavior of the dimensionless average temperature for different dimensionless times, respectively. It is observed in this table an excellent convergence ratio, with practically three digits converged for all positions studied.

Table 1. Convergence behavior of the temperature field at the center of the spheroidal solid ($R = 0, Z = 0$).

τ	NT = 100	NT = 200	NT = 300	NT = 400	NT = 500
$\gamma^{-1} = 0.5$					
0.08	0.3689	0.3687	0.3695	0.3688	0.3688
0.10	0.2499	0.2498	0.2503	0.2498	0.2498
0.20	0.3576×10^{-1}	0.3570×10^{-1}	0.3576×10^{-1}	0.3569×10^{-1}	0.3568×10^{-1}
0.40	0.7320×10^{-3}	0.7300×10^{-3}	0.7300×10^{-3}	0.7280×10^{-3}	0.7280×10^{-3}
0.60	0.1500×10^{-4}				
0.80	0.0000	0.0000	0.0000	0.0000	0.0000
1.00	0.0000	0.0000	0.0000	0.0000	0.0000
$\gamma^{-1} = 2.0$					
0.08	0.9734	0.9735	0.9745	0.9737	0.9738
0.10	0.8557	0.8558	0.8565	0.8560	0.8560
0.20	0.4413	0.4414	0.4416	0.4414	0.4414
0.40	0.1081	0.1081	0.1081	0.1081	0.1081
0.60	0.2546×10^{-1}	0.2546×10^{-1}	0.2547×10^{-1}	0.2546×10^{-1}	0.2546×10^{-1}
0.80	0.5948×10^{-2}	0.5947×10^{-2}	0.5949×10^{-2}	0.5948×10^{-2}	0.5948×10^{-2}
1.00	0.1387×10^{-2}				

Table 2. Convergence behavior of the temperature field at the focal point of the spheroidal solid ($R = L, Z = 0$ for $\gamma^{-1} = 0.5$ and $R = 0, Z = L$ for $\gamma^{-1} = 2.0$).

τ	NT = 100	NT = 200	NT = 300	NT = 400	NT = 500
$\gamma^{-1} = 0.5$					
0.08	0.6386×10^{-1}	0.6380×10^{-1}	0.6390×10^{-1}	0.6379×10^{-1}	0.6381×10^{-1}
0.10	0.4326×10^{-1}	0.4321×10^{-1}	0.4327×10^{-1}	0.4320×10^{-1}	0.4321×10^{-1}
0.20	0.6190×10^{-2}	0.6176×10^{-2}	0.6182×10^{-2}	0.6170×10^{-2}	0.6171×10^{-2}
0.40	0.1270×10^{-3}	0.1260×10^{-3}	0.1260×10^{-3}	0.1260×10^{-3}	0.1260×10^{-3}
0.60	0.3000×10^{-5}				
0.80	0.0000	0.0000	0.0000	0.0000	0.0000
1.00	0.0000	0.0000	0.0000	0.0000	0.0000
$\gamma^{-1} = 2.0$					
0.08	0.2297	0.2269	0.2279	0.2295	0.2297
0.10	0.1715	0.1694	0.1701	0.1713	0.1715
0.20	0.5428×10^{-1}	0.5370×10^{-1}	0.5392×10^{-1}	0.5427×10^{-1}	0.5433×10^{-1}
0.40	0.9658×10^{-2}	0.9558×10^{-2}	0.9597×10^{-2}	0.9659×10^{-2}	0.9669×10^{-2}
0.60	0.2123×10^{-2}	0.2101×10^{-2}	0.2109×10^{-2}	0.2123×10^{-2}	0.2125×10^{-2}
0.80	0.4890×10^{-3}	0.4840×10^{-3}	0.4860×10^{-3}	0.4890×10^{-3}	0.4890×10^{-3}
1.00	0.1140×10^{-3}	0.1120×10^{-3}	0.1130×10^{-3}	0.1140×10^{-3}	0.1140×10^{-3}

Table 3. Convergence behavior of the dimensionless average temperature for different dimensionless times.

τ	NT = 100	NT = 200	NT = 300	NT = 400	NT = 500
$\gamma^{-1} = 0.5$					
0.08	0.1336	0.1335	0.1334	0.1334	0.1334
0.10	0.9059×10^{-1}	0.9045×10^{-1}	0.9040×10^{-1}	0.9037×10^{-1}	0.9035×10^{-1}
0.20	0.1296×10^{-1}	0.1293×10^{-1}	0.1292×10^{-1}	0.1291×10^{-1}	0.1291×10^{-1}
0.40	0.2650×10^{-3}	0.2640×10^{-3}	0.2640×10^{-3}	0.2630×10^{-3}	0.2630×10^{-3}
0.60	0.5000×10^{-5}				
0.80	0.0000	0.0000	0.0000	0.0000	0.0000
1.00	0.0000	0.0000	0.0000	0.0000	0.0000
$\gamma^{-1} = 2.0$					
0.08	0.3484	0.3484	0.3484	0.3484	0.3484
0.10	0.2976	0.2975	0.2975	0.2975	0.2975
0.20	0.1386	0.1386	0.1386	0.1386	0.1386
0.40	0.3162×10^{-1}				
0.60	0.7338×10^{-2}	0.7337×10^{-2}	0.7337×10^{-2}	0.7337×10^{-2}	0.7337×10^{-2}
0.80	0.1709×10^{-2}				
1.00	0.3980×10^{-3}				

Now, it is presented in Figs. (2) and (3) a comparison of the present results among those analytical results presented by Haji-Sheikh and Sparrow (1966) and Haji-Sheikh (1986) and an analytical solution presented by Özisik (1993) for the case of heat conduction in a sphere. From these figures it is observed a good agreement among the results and can also be verified that for $\gamma > 1$ ($L_1 > L_2$ that represents oblate solids) the solid surface $R_w(Z)$, which is subjected to zero temperature, is near to center of the solid and consequently at this point the level of temperature tends to zero more rapidly. On the other hand, as the aspect ratio decreases the temperature at the center is less affected by the boundary condition at surface $R_w(Z)$. It is observed an opposite behavior for the temperature at the focal point.

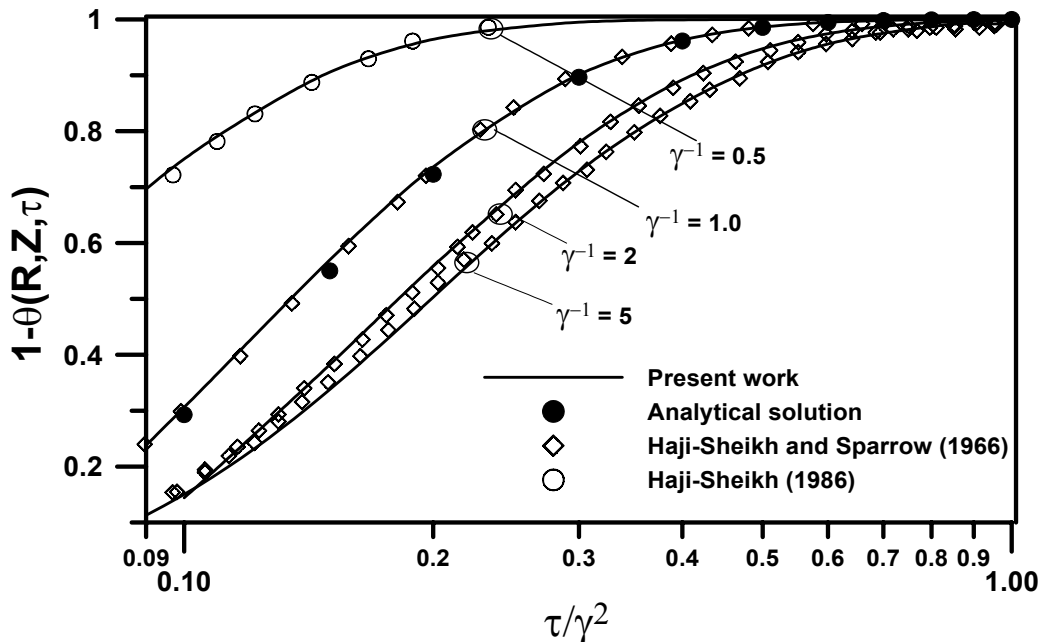


Figure 2. Comparison of the temperature field at the center of the spheroidal solid for different aspect ratios.

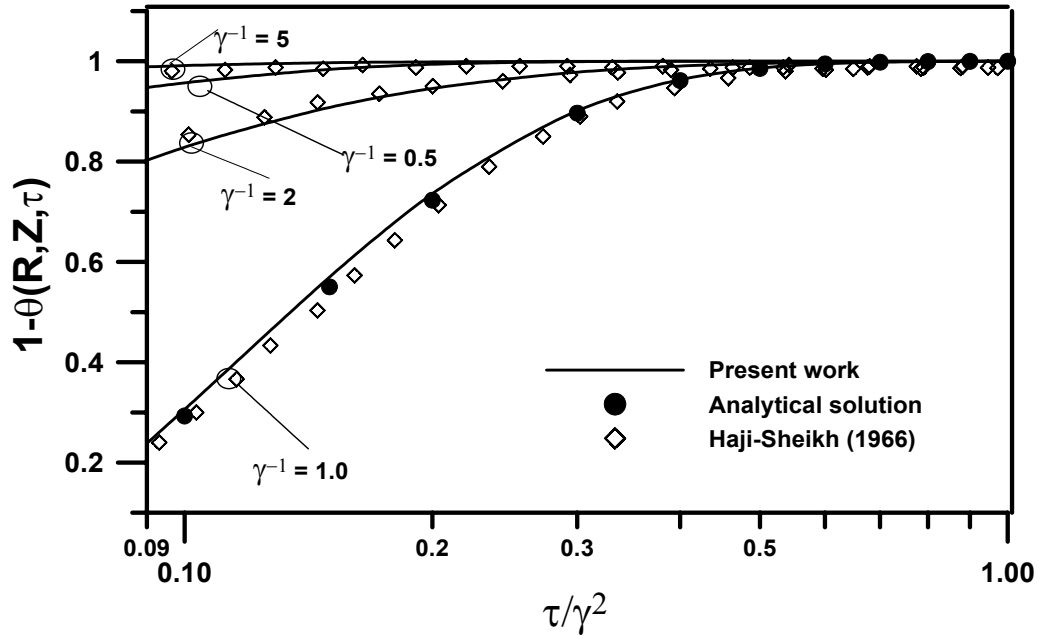


Figure 3. Comparison of the temperature field at the focal point of the spheroidal solid for different aspect ratios.

Finally, Fig. (4) brings the development of the dimensionless average temperature for different aspect ratios and the same observations as the center analysis are verified.

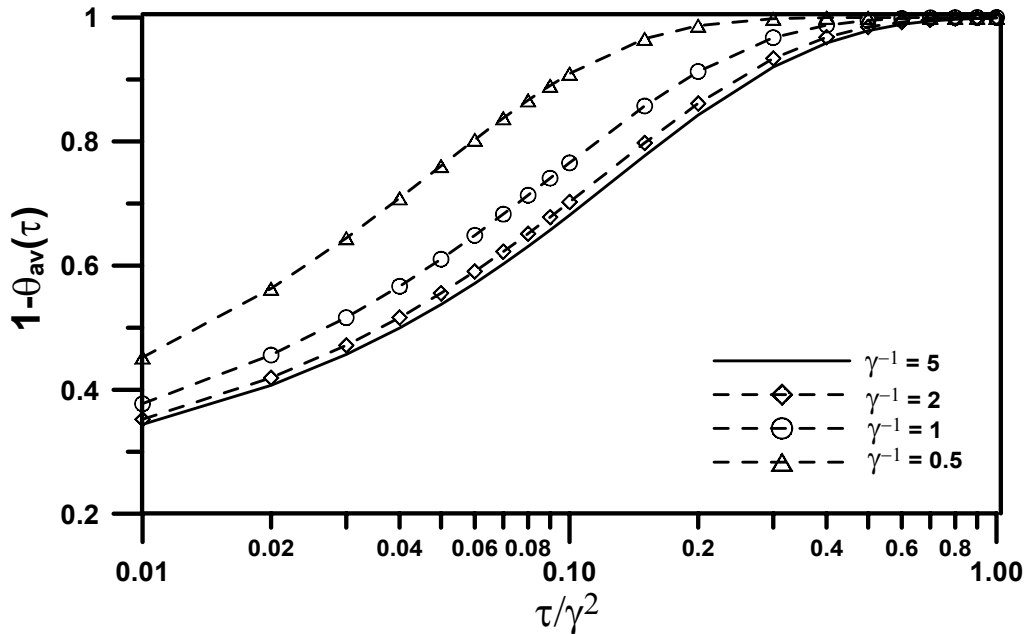


Figure 4. Development of the dimensionless average temperature within the spheroidal solid for different aspect ratios.

4. Conclusions

Numerical results for the temperature field within spheroidal solids with different aspect ratios were produced by using the GITT approach in the solution of the heat conduction equation. Comparisons with previously reported results indicated a good agreement and demonstrating the powerfulness of the GITT approach in handling problems dealing with irregular domains. Also the results indicate that the thermal response at the center point is most rapidly for oblate solids and a inverse behavior is verified at the focal point.

5. References

- Aparecido, J.B., Cotta, R.M. and Özisik, M.N., 1989, "Analytical Solutions to Two-dimensional Diffusion Type Problems in Irregular Geometries", *Journal of the Franklin Institute*, Vol. 326, pp. 421-434.
- Aparecido, J.B. and Cotta, R.M., 1990, "Laminar Flow inside Hexagonal Ducts", *Computational Mechanics*, Vol. 6, pp. 93-100.
- Chaves, C.L., Quaresma, J.N.N., Macêdo, E.N., Pereira, L.M. and Lima, J.A., 2001, "Hydrodynamically Developed Laminar Flow of Non-Newtonian Fluids inside Double-sine Ducts", *Proceedings of the 2nd International Conference on Computational Heat and Mass Transfer*, on CD-ROM, Rio de Janeiro, Brazil, Paper P91.
- Cotta, R.M., 1993, "Integral Transforms in Computational Heat and Fluid Flow", CRC Press, Boca Raton, USA.
- Cotta, R.M., 1994, "Benchmark Results in Computational Heat and Fluid Flow: - The Integral Transform Method", *International Journal of Heat and Mass Transfer*, Vol. 37, pp. 381-394.
- Haji-Sheikh, A. and Sparrow, E.M., 1966, "Transient Heat Conduction in a Prolate Spheroidal Solid", *Journal of Heat Transfer*, Vol. 88, pp. 331-333.
- Haji-Sheikh, A., 1986, "On the Solution of Parabolic Partial Differential Equations Using Galerkin Functions", pp. 467-479, In: *Integral Methods in Science and Engineering*, Hemisphere Publishing Corporation, New York, USA.
- Lima, A.G.B. and Nebra, S.A., 1999, "The Finite-Volume Approach for the Solution of the Transient Diffusion Equation Applied to Prolate Spheroidal Solids", *Proceedings of the 15th Brazilian Congress of Mechanical Engineering – XV COBEM*, on CD-ROM, Águas de Lindóia, Brazil.
- IMSL Library, 1991, MATH/LIB, Houston, TX.
- Pérez Guerrero, J.S., Quaresma, J.N.N. and Cotta, R.M., 2000, "Simulation of Laminar Flow inside Ducts of Irregular Geometry Using Integral Transforms", *Computational Mechanics*, Vol. 25, pp. 413-420.
- Özisik, M.N., 1993, "Heat Conduction", 2nd Ed., Wiley Interscience, New York, USA.